Monthly Notices
of the
ROYAL ASTRONOMICAL SOCIETY

Mon. Not. R. Astron. Soc. **422,** 2187–2194 (2012) doi:10.1111/j.1365-2966.2012.20765.x

Satellites around massive galaxies since $z \sim 2$

E. Mármol-Queraltó,[1,2]★ I. Trujillo,[1,2] P. G. Pérez-González,[3,4] J. Varela[1,2,5] and G. Barro[6]

[1]*Instituto de Astrofísica de Canarias, c/ Vía Láctea s/n, E-38205, La Laguna, Tenerife, Spain*
[2]*Departamento de Astrofísica, Universidad de La Laguna, E-38205, La Laguna, Tenerife, Spain*
[3]*Departamento de Astrofísica, Facultad de CC. Físicas, Universidad Complutense de Madrid, E-28040, Spain*
[4]*Steward Observatory, The University of Arizona 933 N Cherry Avenue, Tucson, AZ 85721, USA*
[5]*Centro de Estudios de Física del Cosmos de Aragón (CEFCA), Plaza San Juan, 1, Planta-2, E44001-Teruel, Spain*
[6]*UCO/Lick Observatory, University of California, Santa Cruz, CA 95064, USA*

Accepted 2012 February 15. Received 2012 January 11; in original form 2011 September 23

ABSTRACT

The accretion of minor satellites has been postulated as the most likely mechanism to explain the significant size evolution of massive galaxies over cosmic time. Using a sample of 629 massive ($M_{\rm star} \sim 10^{11}\,{\rm M}_{\odot}$) galaxies from the near-infrared Palomar/DEEP-2 survey, we explore what fraction of these objects have satellites with $0.01 < M_{\rm sat}/M_{\rm central} < 1$ (1:100) up to $z = 1$ and what fraction have satellites with $0.1 < M_{\rm sat}/M_{\rm central} < 1$ (1:10) up to $z = 2$ within a projected radial distance of 100 kpc. We find that the fraction of massive galaxies with satellites, after background correction, remains basically constant and close to 30 per cent for satellites with a mass ratio down to 1:100 up to $z = 1$, and close to 15 per cent for satellites with a 1:10 mass ratio up to $z = 2$. The family of spheroid-like massive galaxies presents a 2–3 times larger fraction of objects with satellites than the group of disc-like massive galaxies. A crude estimation of the number of 1:3 mergers a massive spheroid-like galaxy has experienced since $z \sim 2$ is around 2. For a disc-like galaxy this number decreases to ∼1.

Key words: galaxies: evolution – galaxies: formation – galaxies: high-redshift.

1 INTRODUCTION

The relevance of major mergers as the main mechanism for the size increase of massive ($M_{\rm star} \gtrsim 10^{11}\,{\rm M}_{\odot}$) galaxies in the last ∼11 Gyr (e.g. Daddi et al. 2005; Trujillo et al. 2006, 2007; Longhetti et al. 2007; Buitrago et al. 2008) is not favoured observationally (e.g. Bundy et al. 2009; de Ravel et al. 2009; López-Sanjuan et al. 2010). This has led to a growing consensus that the significant size evolution observed among massive galaxies is dominated by the continuous accretion of minor satellites. However, all the observational evidence compiled so far suggesting that the merging of minor satellites is the main route of growth in galaxy size is only indirect. The observations that favour the minor merging scenario are: (i) a progressive build-up of the envelopes of massive galaxies over cosmic time (Hopkins et al. 2009; Bezanson et al. 2009; van Dokkum & Brammer 2010; Carrasco, Conselice & Trujillo 2010); and (ii) a mild decrease in the velocity dispersion of these galaxies (e.g. Cenarro & Trujillo 2009; Cappellari et al. 2009; Martinez-Manso et al. 2011; Newman et al. 2010; van de Sande et al. 2011). Both phenomena agree with a process that does not dramatically affect the inner regions of these galaxies. Recently, additional evidence supporting the merging scenario has been provided: the size evolution of massive galaxies is not linked to the age of the stellar population of the galaxies (Trujillo, Ferreras & de La Rosa 2011). All these observations argue against the puffing-up mechanism proposed by Fan et al. (2008, 2010), whereby galaxies grow by the expulsion of gas through the activity of active galactic nuclei, but support the minor merging hypothesis.

From a theoretical point of view, *N*-body cosmological simulations as well as semi-analytical models (e.g. Khochfar & Burkert 2006; Naab, Johansson & Ostriker 2009; Oser et al. 2012) show that the expected accretion rate of satellites should be able to produce a significant increase in the size of the galaxies while at the same time changing the velocity dispersion only mildly. Estimates of the merger rate (e.g. López-Sanjuan et al. 2011) using observations are, however, not straightforward owing to the large uncertainties in the determination of the merging time-scales. Nevertheless, a more direct way of comparing simulations with observations and, consequently, of probing the minor merging scenario is to measure the frequency of satellites found around massive galaxies and quantify how this fraction changes with cosmic time (e.g. Newman et al. 2012; Williams, Quadri & Franx 2011). Several papers have calculated this number in the nearby Universe (see e.g. Chen 2008; Liu et al. 2011). These works show that ∼12 per cent of massive galaxies have at least one satellite with a stellar mass $0.1 < M_{\rm sat}/M_{\rm central} <$

★E-mail: emq@iac.es

1 within a projected radius of 100 kpc. These numbers are in good agreement with expectations from ΛCDM simulations (see e.g. Boylan-Kolchin et al. 2010). de Ravel et al. (2011) and Nierenberg et al. (2011) explored the evolution of the fraction of galaxies with satellites up to $z \sim 1$, but using mostly samples of central galaxies less massive than $10^{11}\,M_{\odot}$. In this paper we concentrate on the most massive galaxies and expand on the previous analysis, exploring the fraction of galaxies with satellites up to $z \sim 2$. To do this, we use a large and complete sample of massive galaxies up to $z = 2$ from Trujillo et al. (2007). We probe two redshift ranges: up to $z = 1$, we explore the fraction of massive galaxies with satellites within the mass range $0.01 < M_{\rm sat}/M_{\rm central} < 1$; and up to $z = 2$, the fraction of massive galaxies with satellites within the mass range $0.1 < M_{\rm sat}/M_{\rm central} < 1$.

This paper is structured as follows. In Section 4 we describe our sample of massive galaxies and the photometric catalogue we used to identify their satellites. Our criteria for selecting satellites as well as our background estimation methods are explained in Section 3. Finally, our results are presented in Section 4, and a discussion of our findings is provided in Section 5. In this paper we adopt a standard ΛCDM cosmology, with $\Omega_{\rm m} = 0.3, \Omega_{\Lambda} = 0.7$ and $H_0 = 70$ km s^{-1} Mpc^{-1}.

2 THE DATA

To analyse the evolution with redshift of the fraction of massive galaxies having satellites, we used as the reference catalogue for central galaxies the compilation of massive objects published in Trujillo et al. (2007) (hereafter T07). This is a homogeneous and large collection of massive galaxies since $z = 2$. Briefly, the sample consists of a total of 831 massive ($M_{\rm star} > 10^{11}\,M_{\odot}$) galaxies (of which 35 were identified as active galactic nuclei and not used subsequently) over 710 arcmin^2 in the Extended Groth Strip (EGS). These objects were $K_{\rm s}$-band-selected in the Palomar Observatory Wide-Field Infrared (POWIR)/DEEP-2 survey (Bundy et al. 2006; Conselice et al. 2007). In total, 372 galaxies have spectroscopic redshifts (Davis et al. 2003), and the remaining redshifts were obtained photometrically using *B, R* and *I* bands from the CFHT 3.6-m telescope, F606W and F814W from the *Hubble Space Telescope*, and *J* and $K_{\rm s}$ from the Palomar 5-m telescope. Stellar masses and other derived photometric parameters were estimated using a Chabrier (Chabrier 2003) initial mass function (IMF). T07 estimated the (circularized) half-light radius ($r_{\rm e}$) and Sérsic indices *n* (Sérsic 1968) for all the galaxies in our sample.

To compile the sample of the satellite galaxies around our massive objects we used the EGS IRAC-selected galaxy sample from the Rainbow Cosmological Data base[1] published by Barro et al. (2011a) (see also Pérez-González et al. 2008). This data base covers an area of 1728 arcmin^2 centred on the EGS and provides spectral energy distributions (SEDs) ranging from the UV to the MIR regime plus well-calibrated and reliable photometric redshifts and stellar masses (Barro et al. 2011b). Around 10 per cent of the galaxies in the Rainbow catalogue have spectroscopic redshifts. From the Rainbow data base we selected all galaxies with $z < 2.2$ and an estimated stellar mass $10^8\,M_{\odot} < M < 10^{12}\,M_{\odot}$. A total of ∼55 000 objects were selected in the EGS area following these criteria. We refer to this resulting sample as the Rainbow catalogue.

The sample of massive galaxies as well as the Rainbow sample were cross-correlated using a 1.0-arcsec search radius to create a sample of central galaxies identified in both catalogues. All the massive galaxies in T07 were found in the Rainbow data base. The average difference between the photometric redshifts for the massive galaxies in the two samples is ∼10 per cent. The average stellar mass of our massive sample according to the Rainbow data set is $0.9 \times 10^{11}\,M_{\odot}$, and is $1.7 \times 10^{11}\,M_{\odot}$ according to T07.

In order to build a sample of central galaxies with the best estimations of redshifts and stellar masses we applied the following rules. (i) If a central galaxy has a spectroscopic redshift determination in Rainbow (348 objects), we used this redshift plus the stellar mass inferred in that catalogue for these two quantities. Among these galaxies, there were eight objects with spectroscopic redshifts in both samples with high discrepancies in the stellar mass estimations from the two catalogues. We reject from our sample such dubious cases. (ii) If no spectroscopic redshift is found in the Rainbow data base but is in the T07 sample (37 galaxies) we use the values of the redshift and stellar masses from that catalogue. (iii) Finally, if no spectroscopic redshift is found in either of the two catalogues we use only those objects for which the photometric redshift determination is robust (317 objects). This means that we have compared the two independent photometric-*z* estimations found in T07 and Barro et al. (2011a) and have taken only those objects for which the photometric redshifts disagree by less than $\Delta z_{\rm phot} = 0.070$ for $0.0 < z < 0.5$, $\Delta z_{\rm phot} = 0.061$ for $0.5 < z < 1.0$, and $\Delta z_{\rm phot} = 0.083$ for $1.0 < z < 2.5$ (typical quality of the photometric-*z*s in the Rainbow catalogue in EGS obtained by comparing them with spectroscopic-*z*s,Barro et al. 2011b). This removes 94 galaxies. For consistency with the sample of satellite galaxies, for these 317 objects we take the stellar masses and photometric redshift from the Rainbow catalogue. After this selection, the number of objects in the final sample of massive galaxies is 694, of which 317 have photometric redshifts from Rainbow and 377 have spectroscopic redshifts (340 from the Rainbow catalogue and 37 from T07).

A final cut in the number of galaxies of our main sample is required to ensure that the fraction of galaxies with satellites along our explored redshift range is not biased by the stellar mass completeness limit of the Rainbow data base. The stellar mass limit (75 per cent complete) of the Rainbow data base at each redshift is provided in Pérez-González et al. (2008, see their fig. 4). In the redshift range $0 < z < 2$ we have selected only those massive galaxies whose stellar masses are 10 times larger than the completeness limit at each redshift. There are 629 galaxies (with a mean stellar mass of $M = 1.3 \times 10^{11}\,M_{\odot}$ for this sample) that meet these criteria. By doing this we are confident that we can explore within the Rainbow catalogue satellites down to a 1:10 mass ratio of the central galaxy in the range $0 < z < 2$. For the same reason, this exercise is done up to $z = 1$, but this time selecting only those central galaxies with a stellar mass 100 times above the mass limit. This cut leaves us with 194 massive galaxies (with a mean stellar mass of $M = 1.7 \times 10^{11}\,M_{\odot}$ in the redshift range $0 < z < 1$). The stellar masses and the redshifts for the central galaxies studied in this work are illustrated in Fig. 1.

3 SELECTION CRITERIA

To identify the satellite galaxies around our central objects we applied the following criteria: (i) we identify all galaxies in the Rainbow catalogue that are within a projected radial distance from our central galaxies of $R_{\rm search} = 100$ kpc (corresponding to 0.3 and 0.2 arcmin for $z = 0.5$ and $z = 2$, respectively); (ii) the difference between their photometric redshifts and the redshift of the central galaxies should be lower than the 1σ uncertainty in the estimation

[1] https://rainbowx.fis.ucm.es/Rainbow_Data base/

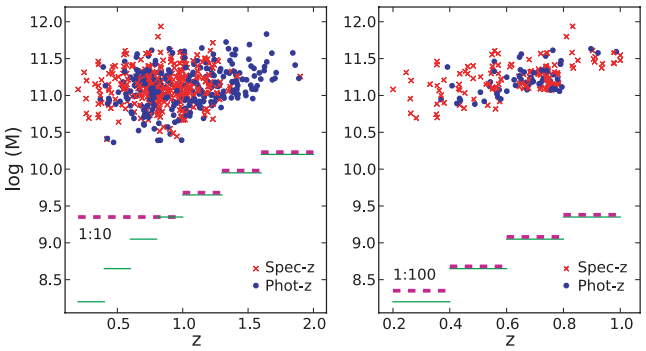

Figure 1. Stellar mass vs. redshift for the massive galaxies analysed in this work. Galaxies with spectroscopic redshifts are plotted in red, while galaxies with photometric estimates are plotted in blue. The left panel shows the distribution of the massive galaxies used for exploring the fraction of galaxies with 1:10 satellites up to $z = 2$. The right panel shows the massive galaxies used in the study of 1:100 satellites up to $z = 1$. The solid green lines illustrate the stellar mass 75 per cent completeness limit of the Rainbow data base for the redshift ranges given in Barro et al. (2011b). The magenta dashed lines show the stellar mass cut used in this paper for the various subsamples.

of the photometric redshifts of the Rainbow data base (i.e. $\Delta z_{\rm phot} = 0.070$ for $0 < z < 0.5$, $\Delta z_{\rm phot} = 0.061$ for $0.5 < z < 1$, and $\Delta z_{\rm phot} = 0.083$ for $1 < z < 2.5$); and (iii) the stellar mass of these objects should be within $0.1 < M_{\rm sat}/M_{\rm central} < 1.0$ for galaxies in the range $0 < z < 2$, and within $0.01 < M_{\rm sat}/M_{\rm central} < 1.0$ for galaxies in the range $0 < z < 1$. An example of a satellite galaxy satisfying the above criteria is shown in Fig. 2. Finally, we consider different redshift bins (see Table 1) to explore the evolution of the fraction, $F_{\rm sat}$, of massive galaxies with satellites. The widths of these bins were chosen to include a similar number of massive galaxies in each bin and to have similar statistics among them.

We adopted a search radius of 100 kpc. This radius is a compromise such that the area is large enough to find a significant number of satellite candidates that are gravitationally bound to our central massive galaxies but not so large that there is severe contamination by background objects. In any case, we have explored the effect on our measurements if we select larger radii of exploration. We computed the fraction of massive galaxies with satellites for various search radii ($R_{\rm search} = 100$, 150, 200 and 250 kpc). The results of this experiment in the mass range $0.1 < M_{\rm sat}/M_{\rm central} < 1$ are shown in Fig. 3. The numbers presented here are corrected for background contamination, as explained later. As expected, we detect an increasing number of massive galaxies with satellites as we expand the search radius $R_{\rm search}$. The only exception is the redshift range $1.1 < z < 2.0$, in which the fraction of massive galaxies with satellites is constant within the error bars. It is worth noting that, in general, beyond $R_{\rm search} = 150$ kpc there is no net increase in the fraction of massive galaxies with satellites. Moreover, our results are basically unchanged if we use a search radius of 100 or 150 kpc. For this reason, in what follows we will present the results based on a search radius of 100 kpc, as our simulations show that this case is affected by the background contamination by a factor of $\sim$2 less than the 150-kpc case.

Similarly to the selection of the search radius, we restricted our potential satellite galaxies to have a redshift difference with the central galaxy not larger than the 1σ uncertainty in the estimation of the photometric redshifts of the Rainbow data base. Larger redshift differences could be used to include more potential candidates, but this is transferred into a larger background contribution to our measurements. For instance, we estimated how the fraction of massive galaxies with satellites changed when using 2σ uncertainty in the estimation of the photometric redshifts instead of 1σ. As expected, we found a slight increase ($\lesssim$30 per cent) in the fraction, but our error bars increased (by 50 per cent) because of the larger amount of background contamination. As these changes do not alter our main results but increase our error bars, we have used the 1σ criterion.

3.1 Background estimation

Despite using photometric redshift information to select our potential satellite galaxies, there is still a fraction of objects that satisfy the above criteria but are not gravitationally bound to our massive galaxies. These objects are counted as satellites because the uncertainties on their redshift estimates place them within our searching redshift range. These foreground and background objects (hereafter we will use the term background to refer to both of them) constitute the main source of uncertainty in this kind of study. Consequently, it is of key importance to estimate accurately the background

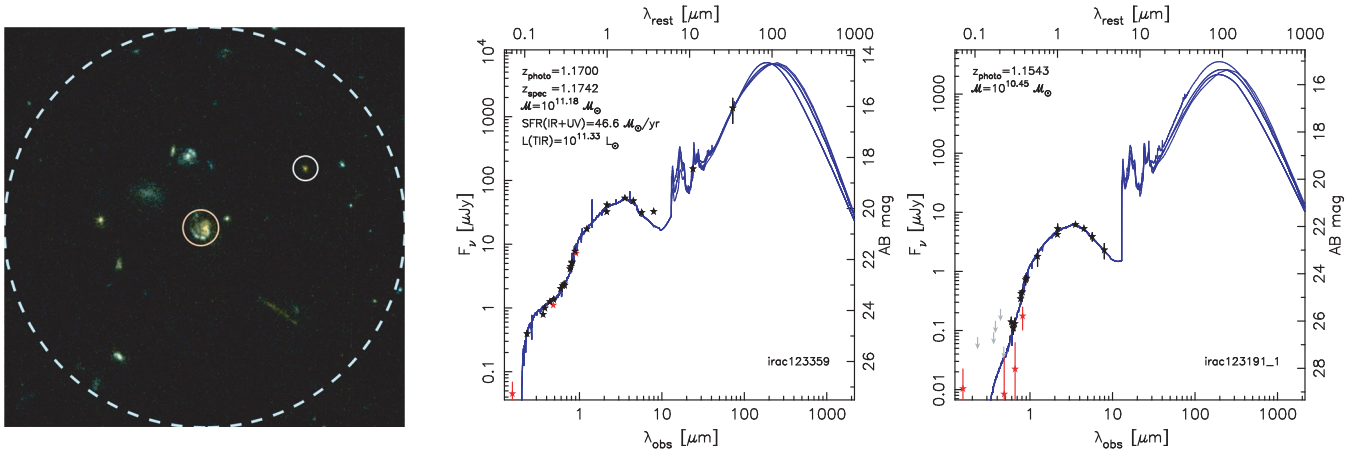

Figure 2. Left panel: ACS colour image of the massive galaxy IRAC123359 (in the centre) at $z = 1.17$, with a satellite galaxy (IRAC123191-1) that meets the selection criteria used in this work enclosed by the white circle. A circle of radius 100 kpc is plotted with a dashed line. Central and right panels: Spectral energy distributions for both the massive (central panel) and the satellite (right) galaxies. These panels also include the redshift and stellar mass estimates according to the Rainbow data base.

Table 1. Fraction of massive galaxies with satellites at various redshifts. For each redshift range we present the number of massive galaxies $N_{\rm central}$ in each bin (number of galaxies with spectroscopic redshifts in brackets), the observed fraction of massive galaxies with satellites $F_{\rm obs}$, the estimate of the background contamination $S_{\rm simul}$, and the estimate of the clustering effect $S_{\rm cluster}$. Finally, we present the final fraction of massive galaxies with satellites when (i) the correction for the background contamination ($F_{\rm sat}$) or (ii) the clustering effect ($F_{\rm cluster}$) is applied.

Redshift range	$N_{\rm central}$ (N with spec z)	$F_{\rm obs}$	$S_{\rm simul}$	$S_{\rm cluster}$	$F_{\rm sat}$	$F_{\rm cluster}$
All galaxies						
$0.10 < M_{\rm sat}/M_{\rm central} < 1.00$						
$0.20 < z < 0.75$	197 (130)	0.29	0.09 ± 0.02	0.15 ± 0.02	0.22 ± 0.02	0.17 ± 0.02
$0.75 < z < 0.90$	129 (76)	0.24	0.10 ± 0.03	0.17 ± 0.03	0.16 ± 0.03	0.08 ± 0.03
$0.90 < z < 1.10$	142 (99)	0.25	0.08 ± 0.02	0.13 ± 0.03	0.18 ± 0.02	0.13 ± 0.02
$1.10 < z < 2.00$	161 (55)	0.18	0.09 ± 0.02	0.09 ± 0.03	0.10 ± 0.02	0.10 ± 0.02
$0.01 < M_{\rm sat}/M_{\rm central} < 1.00$						
$0.20 < z < 0.55$	51 (40)	0.37	0.20 ± 0.06	0.24 ± 0.06	0.22 ± 0.06	0.16 ± 0.06
$0.55 < z < 0.73$	70 (42)	0.53	0.24 ± 0.05	0.36 ± 0.05	0.38 ± 0.05	0.28 ± 0.05
$0.73 < z < 1.10$	73 (53)	0.52	0.27 ± 0.05	0.36 ± 0.06	0.34 ± 0.05	0.25 ± 0.06
Spheroid-like ($n > 2.5$) galaxies						
$0.10 < M_{\rm sat}/M_{\rm central} < 1.00$						
$0.20 < z < 0.75$	137	0.34	0.09 ± 0.03	0.16 ± 0.03	0.28 ± 0.03	0.23 ± 0.03
$0.75 < z < 1.10$	176	0.27	0.08 ± 0.02	0.14 ± 0.04	0.21 ± 0.02	0.15 ± 0.04
$1.10 < z < 2.00$	85	0.18	0.08 ± 0.03	0.08 ± 0.03	0.10 ± 0.03	0.10 ± 0.03
Disc-like ($n < 2.5$) galaxies						
$0.10 < M_{\rm sat}/M_{\rm central} < 1.00$						
$0.20 < z < 0.75$	60	0.18	0.10 ± 0.03	0.15 ± 0.04	0.09 ± 0.03	0.05 ± 0.04
$0.75 < z < 1.10$	95	0.19	0.09 ± 0.03	0.16 ± 0.04	0.10 ± 0.04	0.04 ± 0.04
$1.10 < z < 2.00$	76	0.18	0.09 ± 0.04	0.09 ± 0.05	0.10 ± 0.04	0.11 ± 0.05

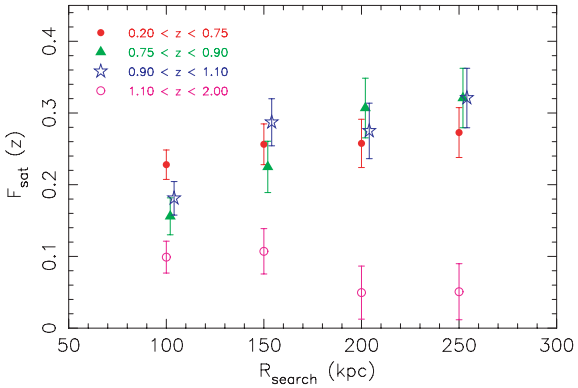

Figure 3. Fraction of massive galaxies having satellites within various projected radial distances (search radius, $R_{\rm search}$) in the mass range $0.1 < M_{\rm sat}/M_{\rm central} < 1.0$ for the various redshift bins studied in this work.

contamination in order to statistically subtract its contribution from the fraction of galaxies with observed satellites.

To estimate the fraction of background sources that contaminate our satellite samples we ran a set of simulations. This method consists of placing a number of mock massive galaxies (equal to the number of our central galaxies) randomly through the volume of the catalogue. To match our observed redshift distribution we ensure that in our simulations the numbers of mock galaxies that are within each redshift bin are the same as in our observed sample. Once we have placed our mock galaxies through the catalogue, we count what fraction of these mock galaxies have satellites around them, taking into account our criteria of redshift and distances explained above. This procedure is repeated two million times to have a robust estimation of the fraction of mock galaxies with satellites. We call this average fraction $S_{\rm simul}$. In addition, these simulations allow us to estimate the scatter in the fraction of galaxies that have contaminants. We use this scatter as an estimation of the error of our real measurements. We consider this fraction to be representative of the background affecting our real central sample. The galaxies in our mock samples keep fixed the parameters of the massive galaxies (i.e. stellar masses and Sérsic indices).

Taking into account that the observed fraction of galaxies with satellites, $F_{\rm obs}$, is the sum of the fraction of galaxies with real satellites, $F_{\rm sat}$, plus the fraction of galaxies that do not have satellites but are affected by contaminants, $(1 - F_{\rm sat}) \times S_{\rm simul}$, we arrive at the following expression:

$$F_{\rm sat} = \frac{F_{\rm obs} - S_{\rm simul}}{1 - S_{\rm simul}}. \quad (1)$$

The results of our simulations are shown in Table 1. From these simulations we see that the fraction $S_{\rm simul}$ of massive galaxies we expect to be contaminated by false satellites (using our searching criteria) is ∼10 per cent for $0.1 < M_{\rm sat}/M_{\rm central} < 1.0$ and ∼25 per cent for $0.01 < M_{\rm sat}/M_{\rm central} < 1.0$.

3.1.1 *Clustering effects*

It is well known that massive galaxies, particularly in the nearby Universe, tend to populate regions that are overdense compared with the average density of the Universe. This implies that there is an excess probability (which we term clustering) of finding galaxies that could be misidentified as satellites of our main targets. It is worth noting that this probability excess is not related to the accuracy of our redshift estimations. Even with all the redshifts measured

spectroscopically, the effect of clustering will be equally relevant in our estimates, as this effect is inherent to our inability to measure real distances but rather to obtain distances inferred by recessional velocities. In massive cluster of galaxies, with a velocity dispersion of $\sim$1000 km s^{-1}, this will limit our accuracy for estimating real galaxy associations.

Because the clustering is a local effect, ideally one would like to measure its influence as close as possible to the central galaxy. In practice, this is done by measuring the amount of satellite candidates in different annuli beyond the search radius (Chen et al. 2006; Liu et al. 2011). We term the fraction of massive galaxies having satellites in these annuli $S_{\rm cluster}$. This fraction measures both the effect of the background contamination and the excess over this background owing to clustering. This method has the disadvantage, compared with the simulations that we have conducted above, that it is statistically more uncertain. $S_{\rm cluster}$ can be measured only around our massive galaxies and this number is relatively small. For this reason, $S_{\rm cluster}$ is determined with an error larger than $S_{\rm simul}$. We count the satellites in nine distinct annuli in the radial range $100 < R < 330$ kpc (the size of each annulus was selected to contain the same area as the searching area within 100 kpc). We find, as expected, that the number of satellites decreases in the outer annuli, reaching asymptotically (within errors) the values we obtain using the first background estimation method. In general, however, and particularly for the lower-redshift bins, the number of detected satellites is higher for the inner annuli than in the random case, and, therefore, the clustering is not negligible. As noted above, the detection of satellites does not increase at $R_{\rm search} > 150$ kpc. For this reason, and as a compromise between proximity to the massive galaxies and having enough statistics, we used the average detections of satellites in the two annuli closer to $R = 150$ kpc ($173 < R < 200$ kpc and $200 < R < 224$ kpc) to estimate the effect of clustering. The uncertainty in measuring $S_{\rm cluster}$ is not straightforward to calculate, and we decided to estimate that value by summing quadratically the background uncertainty measured in the simulations estimating $S_{\rm simul}$ plus the dispersion between the two different radial annuli used in the clustering determination.

The significance of the clustering is quantified in Table 1. We find that above $z > 1$ the clustering plays a minor role as $S_{\rm cluster}$ and $S_{\rm simul}$ are very similar within the errors. At $z < 1$, however, $S_{\rm cluster} \sim 1.5\,S_{\rm simul}$. As expected, the effect of the clustering is more relevant at lower redshifts. At high redshifts, the overdensities are less significant as the large-scale structures are not completely formed.

4 RESULTS

In Table 1 we summarize the results obtained in this work. For each redshift bin, we present the fraction of galaxies with satellites initially found for our sample of massive galaxies, $F_{\rm obs}$, the background estimate $S_{\rm simul}$ derived from the mock catalogues, and the final fraction of massive galaxies with satellites, $F_{\rm sat}$, after correction for the background contamination with equation (1). The associated errors correspond to the standard deviation from the measurements obtained in the mock catalogues as explained in the previous section. In addition, we include the expected contamination arising from the clustering estimate, $S_{\rm cluster}$, and the fraction of massive galaxies with satellites after this correction, $F_{\rm cluster}$.

Our results are also illustrated in Fig. 4. Our main result is seen in the upper left panel of Fig. 4: the fraction of massive galaxies with satellites, within a projected radial distance of 100 kpc, in the range $0.1 < M_{\rm sat}/M_{\rm central} < 1$ remains basically constant (17 ± 3 per cent) in the redshift interval $0 < z < 2$. To have a $z = 0$ comparison, we added the measurement from Liu et al. (2011) using the SDSS sample. They find that at $z = 0$ the fraction of massive galaxies with satellites in the mass range and projected radius explored here is very similar. In the same panel, we show the same analysis up to $z = 1$ for satellite galaxies with $0.01 < M_{\rm sat}/M_{\rm central} < 1.0$. Although slightly noisier owing to the lower statistics, our findings agree with a relatively constant fraction (31 ± 6 per cent) of massive galaxies having such types of satellites.

Our sample of massive galaxies is large enough that we can explore whether the fraction of massive galaxies with satellites in the range $0.1 < M_{\rm sat}/M_{\rm central} < 1$ depends on the morphology of the massive galaxy. We used the Sérsic index as a proxy to the galaxy morphology. In the nearby Universe, galaxies with $n < 2.5$ are mostly disc-like objects, whereas galaxies with $n > 2.5$ are mainly spheroids (e.g. Andredakis, Peletier & Balcells 1995; Blanton et al. 2003; Ravindranath et al. 2004). We used the published Sérsic indexes provided by T07 to separate our galaxies, and illustrate our results in the bottom left panel of Fig. 4. There is a hint that massive galaxies with spheroid-like morphologies tend to have a larger fraction (a factor of 2–3) of galaxies with satellites than disc-like massive objects. This result is more prominent at low redshifts, where the clustering of the massive spheroid population could be an issue.

We can repeat this exercise but this time using the clustering correction (which contains also the background effect) to explore how our results depend on this effect. The comparison between the two types of corrections is shown in Fig. 5. In general, the correction arising from the clustering decreases the fraction of massive galaxies that contain satellites. This fraction is now 12 ± 2 per cent in the redshift interval $0 < z < 2$ for $0.1 < M_{\rm sat}/M_{\rm central} < 1$ and 23 ± 4 per cent for $0.01 < M_{\rm sat}/M_{\rm central} < 1.0$ up to $z = 1$.

4.1 Robustness of the results

The results presented in this paper are the product of combining two data sets: the T07 sample of massive galaxies and the Rainbow catalogue. In addition, we used photometric redshifts and, when available (54 per cent of the time), spectroscopic redshifts. We checked how robust our results are to the use of a more homogeneous data set, by using only a sample of massive galaxies with spectroscopic redshifts or by basing our full analysis on only the Rainbow data base.

In our first test, we used only the central galaxies in our sample with spectroscopic redshifts and determined what fraction has satellites, following the same procedure as explained above and correcting for the background. The widths of the redshift bins for this sample were again chosen to include a similar number of massive galaxies and to have similar statistics to the other samples. The output of this test is shown in Fig. 6. We obtain, for the case of $0.1 < M_{\rm sat}/M_{\rm central} < 1$ up to $z = 2$, an average fraction of 19 ± 4 per cent. It can be seen that this result is in full agreement with our previous estimation for this quantity. In a second test, we took the redshifts and stellar masses only from the Rainbow catalogue to check whether there are systematic effects arising from combining different samples. We have in this case a fraction of 17 ± 2 per cent. Again, this result agrees perfectly with the original estimate. We conclude, accordingly, that our results are robust to both the use of spectroscopic redshifts only and to the mixing of data sets.

Another test that we conducted involved checking whether our results are robust to a change in the stellar mass limit at which our

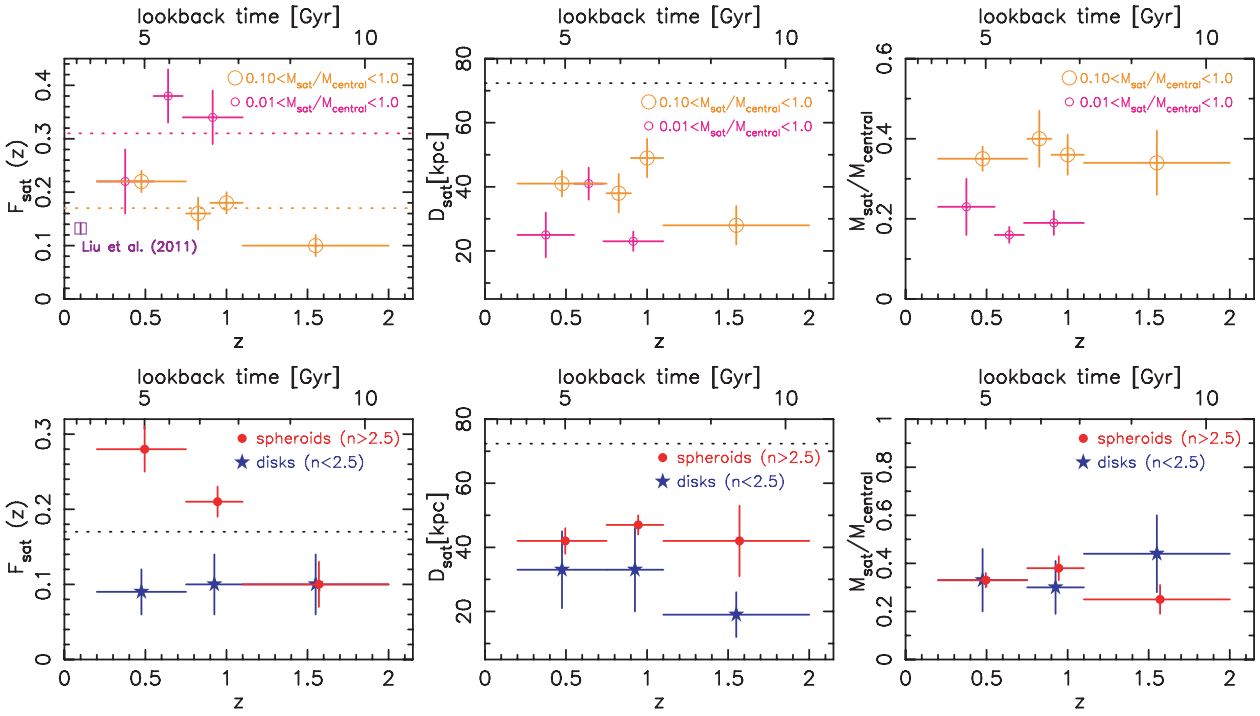

Figure 4. Fraction of massive galaxies having satellites (and their properties) within a projected radial distance of 100 kpc for various redshift bins. Upper panels show the fraction of massive galaxies with satellites in the mass range $0.1 < M_{\rm sat}/M_{\rm central} < 1.0$ (larger orange circles) and the fraction of massive galaxies with satellites in the mass range $0.01 < M_{\rm sat}/M_{\rm central} < 1.0$ (smaller magenta circles). In the bottom panels, we explore the fraction of massive galaxies with satellites in the mass range $0.1 < M_{\rm sat}/M_{\rm central} < 1.0$ when our sample is split depending on the Sérsic index (morphology) of the galaxies (red dots for $n > 2.5$ – spheroids; and blue stars for $n \leq 2.5$ – discs). The horizontal dotted lines in the upper left panel correspond to the average fitted values to our findings. Central panels: Mean projected distances where the satellites are found after statistical correction for the background. The dashed line indicates the average projected distance obtained for mock satellites in the simulations (i.e. this is the expected distance if the satellites are an artefact of the background contamination). Right panels: Mean mass ratios between the satellites and their massive galaxies. The horizontal bars indicate the range of redshifts considered for each measurement. For clarity, we have slightly shifted the data corresponding to spheroid-like objects.

massive galaxies are selected. As illustrated in Fig. 1, the galaxies at higher redshifts are slightly more massive than the bulk of objects at lower redshifts to guarantee that we can study satellites above a given mass ratio along the full redshift range. We checked how our results change if we select only massive galaxies with stellar masses above 2×10^{11} M$_\odot$. We did this exercise for the case $0.1 < M_{\rm sat}/M_{\rm central} < 1$ up to $z = 2$. With the new mass limit, we obtain an average fraction of ∼23 per cent. This is in good agreement with our original estimation for this fraction. Again, increasing the stellar mass limit does not alter substantially the fraction of massive galaxies with satellites.

4.2 Properties of the satellite galaxies

In addition to determining what fraction of the massive galaxies have satellites, we can also estimate the average projected radial distances of these satellites and the average mass ratios between the satellites and the massive objects. To estimate these quantities properly, we need to make statistical corrections for the effect of the contaminants. This can be done using the following expression:

$$\langle Q_{\rm sat}\rangle = \frac{F_{\rm obs}}{F_{\rm sat}}\langle Q_{\rm obs}\rangle - \frac{S_{\rm simul}}{F_{\rm sat}}\langle Q_{\rm simul}\rangle, \quad (2)$$

where $\langle Q_{\rm obs}\rangle$ is the observed mean value of the property Q (i.e. the projected radial distance or the mass ratio), $\langle Q_{\rm simul}\rangle$ is the mean value obtained from the mock massive galaxies (i.e. the values that are found for the contaminants), and $\langle Q_{\rm sat}\rangle$ is the value after the correction.

The mean projected radial projected distances (in kpc) of the satellites and their mean mass ratios $M_{\rm sat}/M_{\rm central}$ are compiled in Table 2 and shown in Fig. 4. We plot with a dashed line the average projected distance (∼72 kpc) of the background galaxies detected as fake satellites in the simulations. After correcting for the effect of the contaminants, we find that our satellite galaxies are at a typical projected radial distance of ∼40 kpc. This value is well below the expectation from a random distribution, suggesting that the satellites are gravitationally bound to their central galaxies. This average distance seems to be largely independent (within errors) of the satellite mass, the morphological type of the central galaxy and the redshift of the system.

Finally, we show in the right panels of Fig. 4 the mean mass ratio $M_{\rm sat}/M_{\rm central}$ in each redshift bin after the statistical correction. We find that $M_{\rm sat}$ is ∼0.36 $M_{\rm central}$ when we explore satellite galaxies within the mass ratio $0.1 < M_{\rm sat}/M_{\rm central} < 1$ (this value is 0.28 when we use the clustering correction). If we explore down to a mass ratio of 0.01, then $M_{\rm sat}$ is ∼0.15 $M_{\rm central}$ (0.14 after correcting for the clustering effect). It is worth noting that, in both cases, the mean masses of our satellites are over 10^{10} M$_\odot$ and consequently we are detecting satellites with large masses. When we split the sample depending on their Sérsic indices (bottom right panel in Fig. 4), there are no significant differences, within the errors, between the

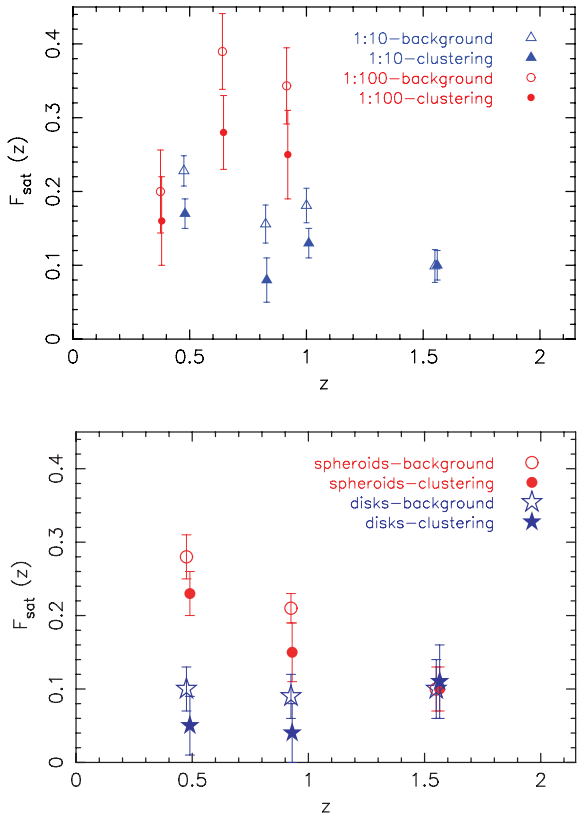

Figure 5. Fraction of massive galaxies with satellites after correction for the background contribution computed from the simulations (open symbols) and when the clustering estimation is used (filled symbols). Top panel: The fraction of massive galaxies with satellites is separated into two groups: $0.1 < M_{\rm sat}/M_{\rm central} < 1.0$ (blue triangles) and $0.01 < M_{\rm sat}/M_{\rm central} < 1.0$ (red circles). Bottom panel: Fraction of massive galaxies in the mass range $0.1 < M_{\rm sat}/M_{\rm central} < 1.0$ depending on the Sérsic index (morphology) of the central galaxies.

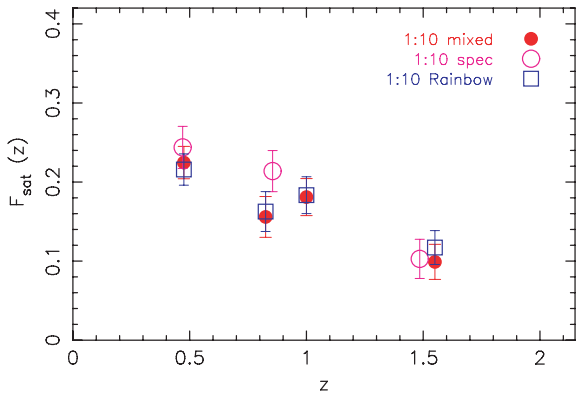

Figure 6. Testing the robustness of the fraction of massive galaxies with satellites in the mass range $0.1 < M_{\rm sat}/M_{\rm central} < 1.0$ for different data sets: our original sample described in Section 2 (solid red circles), a purely spectroscopic sample (magenta circles) and a sample based only on the Rainbow catalogue (blue squares).

two samples. Again we find that the satellites of massive galaxies are similar in their mean properties (distances and mass ratios) independently of the morphological type of their central galaxies and redshift.

Table 2. Mean projected radial distances between the satellites and the central galaxies and their mean mass ratios ($M_{\rm sat}/M_{\rm central}$). These values correspond to the case in which only the background correction has been applied.

Redshift range	Radial distance (kpc)	$M_{\rm sat}/M_{\rm central}$
All galaxies		
$0.10 < M_{\rm sat}/M_{\rm central} < 1.00$		
$0.20 < z < 0.75$	41 ± 4	0.35 ± 0.03
$0.75 < z < 0.90$	38 ± 6	0.40 ± 0.07
$0.90 < z < 1.10$	49 ± 6	0.36 ± 0.05
$1.10 < z < 2.00$	28 ± 6	0.34 ± 0.08
$0.01 < M_{\rm sat}/M_{\rm central} < 1.00$		
$0.20 < z < 0.55$	25 ± 7	0.23 ± 0.07
$0.55 < z < 0.73$	41 ± 5	0.16 ± 0.02
$0.73 < z < 1.00$	23 ± 3	0.19 ± 0.03
Spheroid-like ($n > 2.5$) galaxies		
$0.10 < M_{\rm sat}/M_{\rm central} < 1.00$		
$0.20 < z < 0.75$	42 ± 4	0.33 ± 0.03
$0.75 < z < 1.10$	47 ± 3	0.38 ± 0.05
$1.10 < z < 2.00$	42 ± 11	0.25 ± 0.06
Disc-like ($n < 2.5$) galaxies		
$0.10 < M_{\rm sat}/M_{\rm central} < 1.00$		
$0.20 < z < 0.75$	33 ± 12	0.33 ± 0.13
$0.75 < z < 1.10$	33 ± 13	0.30 ± 0.11
$1.10 < z < 2.00$	19 ± 7	0.44 ± 0.16

5 DISCUSSION AND CONCLUSIONS

The results of this paper support a picture in which the fraction of massive ($M_{\rm star} \sim 10^{11}\,{\rm M}_{\odot}$) galaxies with satellites, within a projected radius of 100 kpc, has not changed with time since $z \sim 2$. This fraction remains about ∼15 per cent for galaxies with satellites with mass $M_{\rm star} \gtrsim 10^{10}\,{\rm M}_{\odot}$ and about ∼30 per cent if we explore satellites with masses $M_{\rm star} \gtrsim 10^{9}\,{\rm M}_{\odot}$ up to $z = 1$.

Interestingly, there is a hint that the fraction of massive galaxies with satellites is larger (by a factor of around 2 to 3) for those galaxies with spheroid-like morphologies than for galaxies with a disc-like appearance (very evident for $z \lesssim 1.1$). This fact could be linked to the different size growth we observe for these two types of objects with cosmic time. In fact, spheroidal galaxies are known for growing more dramatically in size since $z \sim 3$ than disc galaxies (see e.g. T07; Buitrago et al. 2008). It could also be possible that the difference in the fraction of galaxies with satellites between spheroidal and disc-like galaxies is just an effect of the clustering, more relevant at lower redshifts (Section 3.1.1). However, this difference remains even when this effect is taken into account (Fig. 5). We note, however, that it is difficult to correct the clustering effect accurately. With the present data set, a mild redshift evolution of the fraction of spheroid-like galaxies with satellites cannot be excluded.

Owing to the enormous uncertainty on the merging time-scales (e.g. Lotz et al. 2011), it is beyond the scope of this work to estimate a robust merger rate associated with our measurements. Nonetheless, we can make a crude estimation of the number of mergers a massive galaxy has experienced since a given z according to the following expression: $N_{\rm m} = T(z)\,F_{\rm sat}/\tau_{\rm m}$, where $T(z)$ is the interval of cosmic time since a given z until now, and $\tau_{\rm m}$ is the merging time-scale of the satellite within a given radius. For each massive galaxy at $z = 2$ and assuming $\tau_{\rm m} \sim 1.5$ Gyr (e.g. Lotz et al. 2011), we would expect that the number of mergers with a mass ratio of

about 1:3 would be ∼1 (∼2 in the case of a spheroid-like galaxy) since that epoch. For a massive galaxy at $z = 1$, we would expect that the number of mergers with a mass ratio of about 1:6 would be ∼1.5 since that redshift. Again, these numbers are uncertain and very much dependent on the exact merging time-scale, which is a function of the baryonic mass ratio and the model used to estimate this quantity (e.g. Bluck et al. 2009; Conselice, Yang & Bluck 2009; Lotz et al. 2011; Williams et al. 2011; Man et al. 2012). These numbers of mergers are, however, slightly lower (although the exact number is difficult to quantify) than the expected number of mergers obtained using theoretical recipes for the size increase of a galaxy after a merger (see Trujillo et al. 2011). Recently, Bluck et al. (2012) found that a massive galaxy ($M_{\rm star} > 10^{11}\,{\rm M}_{\odot}$) will experience on average $N_{\rm m} = (1.1 \pm 0.2)/\tau_{\rm m}$ minor mergers over the redshift range $z = 1.7 - 3$. This would mean a final $N_{\rm m} \sim 1$ using the $\tau_{\rm m}$ considered in our work. If this is confirmed, it will point to the possibility that the merging activity at those redshifts would be higher than that at lower redshifts. When the results are extrapolated in redshift, these authors find a total final number of minor mergers of $N_{\rm m} = (4.5 \pm 2.9)/\tau_{\rm m}$ from $z = 3$, although, once more, the large errors make it very difficult to constrain the final number of experienced mergers.

At present, there are a few cosmological simulations in which the size growth of the massive galaxies is explained by the accretion of minor satellites (see Naab et al. 2009; Oser et al. 2012). It would be straightforward to compare our findings with these cosmological simulations of galaxy formation and to check whether the fractions that we find are recovered in such theoretical analyses. If this were the case, support for minor merging as the main mechanism responsible for the size evolution of massive galaxies would be greatly enhanced.

ACKNOWLEDGMENTS

We thank the anonymous referee for a careful and constructive reading of the manuscript that helped us to improve the quality of the paper. We are grateful to Lulu Liu for providing us with their measurements of the fraction of galaxies with satellites obtained from the SDSS, used here as a local ($z = 0$) comparison. We thank Juan Betancort for his valuable input on several aspects of the statistical analysis in this paper. We are grateful to Sergio Pascual for his very useful help with programming questions. We would like also to acknowledge fruitful discussions with Javier Cenarro, Luis Díaz, Rosa Domínguez, Cesar González, Carlos López-San Juan, José Oñorbe, Thorsten Naab and Vicent Quilis. IT is a Ramón y Cajal Fellow of the Spanish Ministry of Science and Innovation. This work has been supported by the 'Programa Nacional de Astronomía y Astrofísica' of the Spanish Ministry of Science and Innovation under grant AYA2010-21322-C03-02. PGP and GB acknowledge support from the Spanish Programa Nacional de Astronomía y Astrofísica under grants AYA2009-10368 and AYA2009-07723-E. This work has made use of the Rainbow Cosmological Surveys Data base, which is operated by the Universidad Complutense de Madrid (UCM).

REFERENCES

Andredakis Y. C., Peletier R. F., Balcells M., 1995, MNRAS, 275, 874
Barro G. et al., 2011a, ApJS, 193, 13
Barro G. et al., 2011b, ApJS, 193, 30
Bezanson R., van Dokkum P. G., Tal T., Marchesini D., Kriek M., Franx M., Coppi P., 2009, ApJ, 697, 1290
Blanton M. R. et al., 2003, ApJ, 594, 186
Bluck A. F. L., Conselice J., Bouwens R., Daddi E., Dickinson M., Papovich C., Yan H., 2009, MNRAS, 394, L51
Bluck A. F. L., Conselice J., Buitrago F., Gruetzbauch R., Hoyos C., Mortlock A., Bauer A. E., 2012, ApJ, 747, 34
Boylan-Kolchin M., Springel V., White S. D. M., Jenkins A., 2010, MNRAS, 406, 896
Buitrago F., Trujillo I., Conselice C. J., Bouwens R. J., Dickinson M., Haojing Y., 2008, ApJ, 687, L61
Bundy K., Fukugita M., Ellis R. S., Targett T.A., Belli S., Kodama T., 2006, ApJ, 697, 1369
Bundy K. et al., 2009, ApJ, 651, 120
Cappellari M. et al., 2009, ApJ, 704, L34
Carrasco E. R., Conselice C. J., Trujillo I., 2010, MNRAS, 405, 2253
Cenarro A. J., Trujillo I., 2009, ApJ, 696, L43
Chabrier G., 2003, PASP, 115, 763
Chen J., 2008, AJ, 484, 347
Chen J., Kravtsov A. V. et al., 2006, ApJ, 647, 86
Conselice C. J. et al., 2007, MNRAS, 381, 962
Conselice C. J., Yang C., Bluck A. F. L., 2009, MNRAS, 394, 1956
Daddi E. et al., 2005, ApJ, 626, 680
Davis M. et al., 2003, Proc. SPIE, 4834, 161
van Dokkum P. G., Brammer G., 2010, ApJ, 718, L73
Fan L., Lapi A., De Zotti G., Danese L., 2008, ApJ, 689, L101
Fan L., Lapi A., Bressan A., Bernardi M., De Zotti G., Danese L., 2010, ApJ, 718, 1460
Hopkins P. F., Hernquist L., Cox T. J., Keres D., Wuyts S., 2009, ApJ, 691, 1424
Khochfar S., Burkert A., 2006, AJ, 445, 403
Liu L., Gerke B. F., Wechsler R. H., Behroozi P. S., Michael T., 2011, ApJ, 733, 62
Longhetti M. et al., 2007, MNRAS, 374, 614
López-Sanjuan C., Ballcels M., Pérez-González P. G., Barro G., García-Dabó C. E., Gallego J., Zamorano J., 2010, ApJ, 710, 1170
López-Sanjuan C., 2011, A&A, 530, 20
Lotz J. M., Jonsson P., Cox T. J., Croton D., Primack J. R., Somerville R. S., Sewart K., 2011, ApJ, 742, 103
Man A. W. S., Toft S., Zirm A. W., Wuyts S., van der Wel A., 2012, ApJ, 744, 85
Martinez-Manso J. et al., 2011, ApJ, 738, 22
Naab T., Johansson P. H., Ostriker J. P., 2009, ApJ, 699, L178
Newman A. B., Ellis R. S., Treu T., Bundy K., 2010, ApJ, 717, L103
Newman A. B., Ellis R. S., Bundy K., Treu T., 2012, ApJ, 746, 162
Nierenberg A. M., Auger M. W., Treu T., Marshall P.J., Fassnacht C. D., 2011, ApJ, 731, 44
Oser L., Naab T., Ostriker J. P., Johansson P. H., 2012, ApJ, 744, 630
Pérez-González P. G. et al., 2008, ApJ, 675, 234
de Ravel L. et al., 2009, A&A, 498, 379
de Ravel L. et al., 2011, A&A, submitted (arXiv:1104.5470)
Ravindranath S. et al., 2004, ApJ, 604, L9
van de Sande J., Kriek M. et al., 2011, ApJ, 736, L9
Sérsic J. L., 1968, Atlas de Galaxias Australes Observ. Astronomico, Córdoba
Trujillo I. et al., 2006, ApJ, 650, 18
Trujillo I., Conselice C. J., Bundy K., Cooper M.C., Eisenhardt P., Ellis R.S., 2007, MNRAS, 382, 109
Trujillo I., Ferreras I., de La Rosa I.G., 2011, MNRAS, 415, 3903
Williams R. J., Quadri R. F., Franx M., 2011, ApJ, 738, L25

This paper has been typeset from a TEX/LATEX file prepared by the author.